A Dynamic Spot Diffusing Architecture for Indoor Wireless Optical Communications

Farhad Khozeimeh and Steve Hranilovic
Department of Electrical and Computer Engineering, McMaster University
Hamilton, Ontario, L8S 4K1 Canada
Email: khozeimeh@grads.ece.mcmaster.ca, hranilovic@mcmaster.ca

***Abstract*— In this work we introduce a novel high-speed architecture for indoor wireless optical communications termed the *dynamic spot diffusing* (DSD) architecture. In this configuration the transmitter modulates data onto a spot on the ceiling which moves in a closed path. An imaging receiver acquires data whenever the transmitter spot is in its field-of-view (FOV). We show that this technique is more flexible, has greater multipath immunity, permits higher data rates and has a simpler transmitter than previously defined multi-spot and diffuse architectures. We compare the available channel capacities for a family of spot paths and receiver FOV. Instead of synchronizing to the spot location, rateless erasure correcting codes are applied to approach the capacity of the simulated DSD links. In a $6\times6\times3$ m room, simulated data rates vary between 12.1 Mbps to 40 Mbps at different positions using a single 100 Mbps transmitter and the designed erasure correction code.**

I. Introduction

Indoor high-speed wireless applications have grown rapidly and wireless optical networks have gained attention as a potential solution. In the optical band, there is a wealth of bandwidth that is unregulated world-wide making it theoretically possible to have very high-speed communications. However, indoor wireless optical transmissions are limited due to low-pass multipath distortion and limited average optical power due to eye and skin safety issues. As a result, much effort has been expended to develop optimized channel architectures to realize higher data rates. In this paper, we introduce the *dynamic spot diffusing* (DSD) wireless optical channel. This channel architecture is shown to overcome the multipath and optical power limitations of the indoor channel and provide high data rates with a relatively simple transmitter and erasure correction coding.

Diffuse wireless optical channels emit radiation over a large solid angle while the receivers collect the reflected power with a wide field-of-view (FOV) detector [1]. This configuration permits a great deal of mobility and robustness to blocking and shadowing, however, data rates are limited due to intense multipath distortion. Standard IrDA advanced infrared (AIr) links support data rates of at most 4 Mbps [2] while IEEE 802.11 diffuse links support maximum rates of 2 Mbps [3]. On the other hand, directed line-of-sight wireless optical links enjoy high data rates at the cost of precise alignment between transmitter and receiver.

The multispot diffusing (MSD) architecture combines the benefits of directed and diffuse links [5, 6]. In MSD networks, the transmitter sends data by modulating several narrow beams to create an array of spots on the ceiling. Ideally, a receiver images a single spot and decodes the transmitted data. Identical data is transmitted to all spots in a room. Computer generated holograms have been proposed to form arrays of 10×10 spots for this application [7]. MSD receivers have a smaller FOV than diffuse links and thus collect less multipath distortion. Simulated bandwidths for MSD links are in excess of 2 GHz [8]. Recent work considers a line strip arrangement for the spots which still offers significant gains over diffuse links at a lower complexity [9].

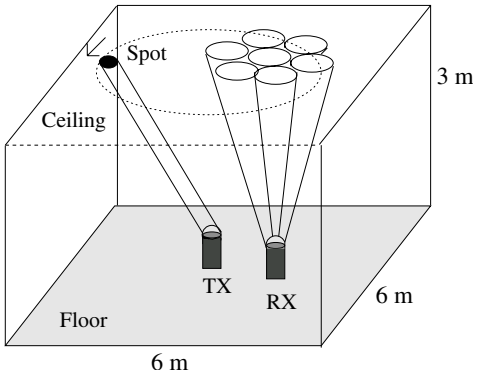

Fig. 1: The proposed DSD configuration

The *dynamic* spot diffusing architecture proposed here derives many of the advantages of MSD links while reducing the complexity of the transmitter. As shown in Fig. 1, the DSD channel configuration consists of a single spot which is translated over the ceiling in a closed path. A multi-element imaging receiver is directed towards the ceiling and performs select-best combining [10]. Data symbols are received whenever the transmitted beam is in the FOV of the receiver. As discussed in [8], the main limitation of MSD channel bandwidth are receptions from more than one spot in the receiver FOV. This is not a problem in the DSD channel since there is a single (or few) optical emitters which greatly reduces the impact of multipath distortion over MSD, allowing for the use of a high speed modulator. The channel capacity of this link is computed and shown to provide high data rates. In order to realize the channel capacity, we apply a class of erasure correcting codes termed *rateless codes* to this channel. Due to the robustness of these codes, user mobility is permitted while maintaining the highest possible rate for any given point in a

1-4244-0355-3/06/$20.00 (c) 2006 IEEE

This full text paper was peer reviewed at the direction of IEEE Communications Society subject matter experts for publication in the IEEE ICC 2006 proceedings.

room. Simulations indicate that with a 100 Mbps modulator data rates as high as 40 Mbps are available at the receiver using a single low complexity transmit beam.

The paper starts with a formal definition of the DSD channel in Sec. II and presents a discussion on transmitter and receiver design as well as on path selection. In Sec. III erasure correcting codes are presented as a practical solution which approaches the capacity of the DSD channel. Finally, the paper concludes in Sec. IV with directions for future work.

II. The Dynamic Spot Diffusing Channel

In a DSD system a few or even a single spot moves on the ceiling with a specific path such as a circle or a line in a periodic manner and is modulated with high bit rate data. As shown in Fig. 1, the receiver consists of multiple imaging elements oriented toward the ceiling. There are many examples of such imaging receivers for indoor wireless optical channels [4, 10, 20]. Each receiver receives data whenever the spot is in its field of view and receives only noise when the spot is not in its field of view.

Unlike MSD wireless optical links, the channel characteristics to any one receiver vary greatly in time, even for stationary receivers. The channel alternates between two states: a wide bandwidth high SNR channel when the spot is in the FOV of the receiver and a very low data rate, poor SNR link otherwise. In fact, the spot motion adds a degree of *fading* to this wireless optical channel. The advantage, however, of the spot motion is the added flexibility of the channel and simple transmitter design. The data rate for this channel will be shown to be quite high, in excess of 20 Mbps using a low complexity 100 Mbps transmitter. Rather than trying to synchronize the receiver to the transmitter we design channel coding techniques which approach this rate in Sec. III.

This section presents a discussion on the characteristics of the DSD channel and on the design of transmitter, receiver and the selection of spot path. The goal of design is to engineer a channel which provides high data rates to all parts of a room.

A. DSD Channel Model

Indoor wireless optical channels can be well represented as the baseband channel [11],

$$y(t) = x(t) \otimes h(t) + n(t) \tag{1}$$

where $\otimes$ denotes convolution, $y(t)$ is the received photocurrent, $x(t)$ is the transmitted intensity, $h(t)$ is the channel impulse response and $n(t)$ is the channel noise.

Indoor wireless optical channels are impaired by strong ambient illumination which results in high-intensity shot noise. The noise, $n(t)$, is modeled as white, independent of the transmitted signal and Gaussian distributed [11, 12]. Since $x(t)$ is an optical intensity, all amplitudes must be non-negative and the average amplitude is constrained for eye-safety. In this work, we assume that rectangular on-off keying is the modulation used for the DSD link.

The channel response, $h(t)$, in (1) can be separated into two components

$$h(t) = h_{\mathrm{LOS}}(t) + h_{\mathrm{MUL}}(t) \tag{2}$$

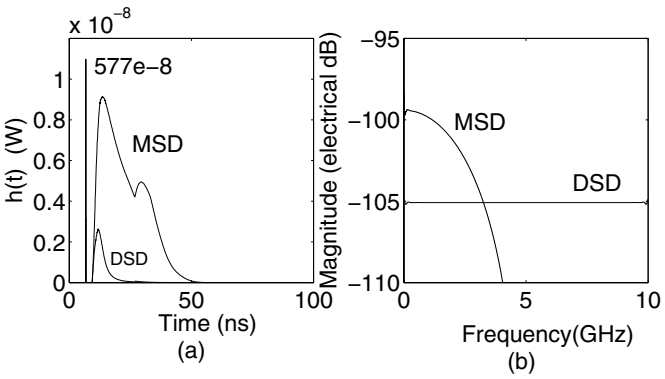

Fig. 2: (a) Received multipath signal for an MSD and DSD system with receiver $FOV = 11.2°$, (b) Frequency response for MSD and DSD systems.

where $h_{\mathrm{LOS}}(t)$ is due to the line-of-sight (LOS) path and $h_{\mathrm{MUL}}(t)$ is due to multipath distortion. In order to compare the multipath distortion of a DSD system versus an MSD channel [8], the impulse response was simulated using the well-known technique of Barry *et al.* [13]. For both simulations the room size was $6 \times 6 \times 3$ m and the receiver was placed at a height of 1 m from the floor. A 10×10 array of equal power spots was used for the MSD channel, as in [8], and the DSD channel was simulated for a single spot centered in the receiver FOV with power equal to a single MSD spot. In both cases, the receiver FOV was set to $11.2°$ as in [8]. Fig. 2 plots the $h(t)$ and the frequency response of the DSD and MSD channels. Notice that the multipath component of MSD is much larger than DSD channels due to the increased number of spots. Since there are two spots in the MSD receiver FOV, the 3 dB bandwidth of the MSD channel is near 2.4 GHz while the DSD channel bandwidth exceeds 10 GHz, however the MSD DC gain is larger than the DSD channel in this simulation. Thus, as noted previously for the MSD channel [6, 7], the DSD channel is "virtually multipath free" and is characterized by a time-varying gain at each point in the room.

The key difference between the DSD channel and other indoor diffuse channels is the time-varying nature of $h(t)$. Because of the wide bandwidth of the DSD channel response, we approximate the frequency response to be flat in the band of interest. Figure 3(a) plots the channel gain for a single period of spot motion for four points in the room, shown in Fig. 3(b), when the spot follows a circular path with period T seconds. The receiver in the simulation is an imaging receiver with FOV of $45°$ such as the one presented in [10]. Notice that the channel gain for each position is nearly flat and is either near zero or has some positive gain, corresponding to times when the spot is outside or inside the receiver FOV. Let $\Delta t(x, y)$ be the length of time that the transmit spot is in the FOV of a receiver at position (x, y) for a single period. Define the *channel duration* at point (x, y) as

$$C_T(x, y) = \Delta t(x, y)/T.$$

A *blind point* is defined as a point in the room for which

This full text paper was peer reviewed at the direction of IEEE Communications Society subject matter experts for publication in the IEEE ICC 2006 proceedings.

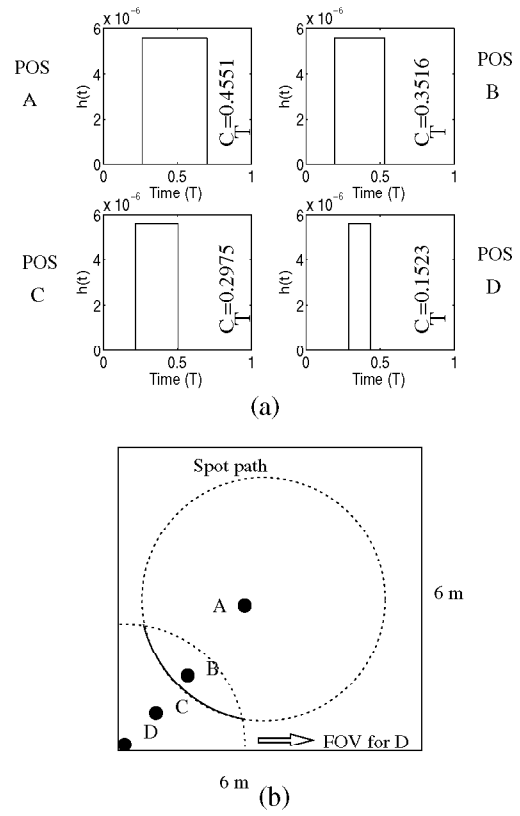

Fig. 3: Variation of channel gain for one period of spot motion (a) at various locations in the room (b).

$C_T = 0$. Data transmission is only possible during times when the spot is in the FOV of the receiver. Thus, to a good approximation, this channel behaves as an *erasure* channel which either transmits the message without distortion or erases it. The channel capacity of such an erasure channel with erasure probability $1 - C_T$ is in fact C_T [14]. Although this is not a rigorous argument for the channel capacity, numerical simulations using the simulated channel and noise estimate from [9] indicate that it is a good approximation. Thus, the goal of DSD channel design is to provide large C_T at all points in a room to ensure large available rates to all users.

B. DSD System Design

The transmitter of the DSD system can be realized using a high-speed laser source with a diffuser. In this work, we assume that the transmitter is able to modulate on-off keyed data at rates of 100 Mbps, such as the one proposed in [10]. The translation of the transmitter spot can be accomplished by rotating the transmitter or by using commercial scanners for bar code reading applications [15].

The design of the receiver is of critical importance in determining the capacity of DSD systems. Imaging receivers have many inherent advantages over single element receivers due to the fact that they can reject spatially localized noise and interference due to their large number of narrow FOV pixels [10]. Thus, the total FOV of an imaging receiver can be large and consists of many narrow FOV pixels. In this work, we assume that the receiver is an imaging receiver consisting of 37 pixels with total FOV of 45° as reported in [10].

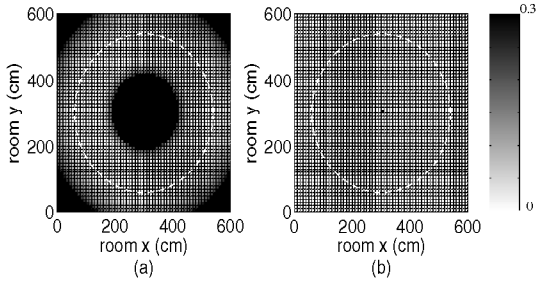

Fig. 4: C_T distribution over the room for (a) FOV=30° and (b) FOV=45°.

FOV	30°	45°
Average C_T	0.1067	0.3312
Variance	14.02	16.21
Max C_T	0.1697	0.4683
Blind points	20.13 %	0.02 %

TABLE I: DSD channel characteristics over receiver FOV

Combining over the received elements is required to improve the detection fidelity. Although maximal-ratio combining (MRC) is optimum in the sense of maximizing SNR, in this paper we consider *select-best combining* (SBC). In this technique, the receiver outputs the element which has the best SNR. It has been shown that for less than 100 elements, MRC and SBC have nearly identical performance [10]. Thus, we select SBC due to its simple implementation and relatively good performance for small to moderate sized receive arrays.

C. Receiver Field-of-View

The capacity of the DSD channel is dramatically dependent on the receiver FOV and the spot path. In Sec. II-D, the capacities of several spot paths are compared for a given receiver FOV. In this section, we quantify the impact of receiver FOV on C_T.

For a given spot path, increasing the receiver FOV improves the duration over which the spot can be detected. Notice, for a fixed pixel size, in order to increase the FOV and not increase the noise or multipath components, the number of imaging elements must also increase using SBC. Thus, in order to maximize the capacity of DSD channels wide FOV imaging receivers with multiple elements should be employed. Fig. 4 plots the C_T for various positions in the prototype room for a circular spot path of radius 2.4 m. As expected, the maximum capacities occur near the spot path with blind spots far off the path. Table I presents the key parameters of the DSD channel with 30° and 45° receiver FOVs assuming a large number of narrow FOV receive elements. The results indicate that with a FOV of 45° that the average and maximum capacity, C_T, is over three times that of the 30° FOV channel and the proportion of blind points decreases from over 20.13% to 0.02%.

D. Path Selection

The selection of the spot path is another important issue affecting the capacity of DSD channels. In this section, the

This full text paper was peer reviewed at the direction of IEEE Communications Society subject matter experts for publication in the IEEE ICC 2006 proceedings.

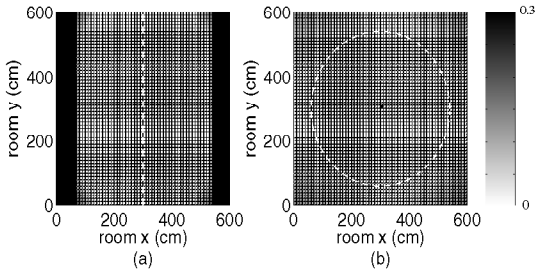

Fig. 5: Distribution of C_T over the room for (a) line and (b) circle radius=2.4 m paths (paths shown in white dashed line and FOV=45°)

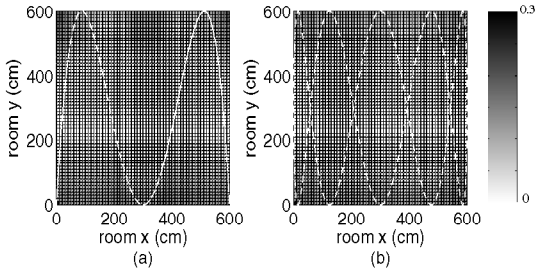

Fig. 6: Distribution of C_T over the room for Lissajou figures with $\omega_x = 1$ and (a) $\omega_y = 4$, (b) $\omega_y = 5$ paths (paths shown in white dashed line and FOV=45°)

distribution of C_T over the room is simulated for several candidate paths assuming an imaging receiver with 45° FOV. A valid path for the DSD channel is any closed path on the ceiling. In Fig. 5 the C_T distribution over the room is plotted for two simple paths, namely, a line and a circle. Another possible family of closed paths are *Lissajou paths*. These paths can be defined as a function of time as

$$\begin{aligned} x &= A(\sin(2\pi\omega_x t/T)+1) \quad [\text{cm}] \\ y &= B(\cos(2\pi\omega_y t/T)+1) \quad [\text{cm}]. \end{aligned}$$

In the case of our prototypical room, we consider the case where $A = B = 300$ cm, $\omega_x = 1$ with $\omega_y = 4$ or $\omega_y = 5$. Fig. 6 presents these paths as well as their C_T distributions.

Table II compares the DSD channel characteristics of the four different paths. The circular path is selected as the best path of the four considered. The period of this path, at a 10 m/s beam speed, is among the smallest reducing the latency of communication and the buffering required for channel coding, discussed in Sec. III. In fact, due to the simple path shape, a laser source could be rotated at higher rates reducing latency even further. The average and maximum capacity, C_T, over all points in the room is highest for the circular path. The number of blind points is also small for this path. An important feature of the circular path is the low variance in C_T over the room. The goal of path design is to have a "fair" channel which provides high capacities throughout

Path	Line 5(a)	Circle 5(b)	Lissajou 6(a)	Lissajou 6(b)
T (s)	1.2	1.5	4.76	5.9
Avg C_T	0.2751	0.3312	0.2153	0.2151
Variance	254.95	16.21	17.25	16.81
Max C_T	0.645	0.4683	0.3009	0.2866
Blind points	36.07 %	0.02 %	0 %	0 %

TABLE II: Channel characteristics for four different spot paths (FOV=45°)

the room. Therefore, circular spot paths have the potential to provide high C_T links at nearly all points in a room. This path is mechanically simple to implement and can be adapted to different sized rooms by altering the radius of the path or its eccentricity creating elliptical path shapes.

III. Channel Coding

As shown in Sec. II, the DSD channel is well approximated as an erasure channel with erasure probability $1-C_T$. In order to approach the channel capacity, an erasure correcting code must be developed for all positions in the room.

Reed-Solomon (RS) codes are among the most popular erasure correcting codes with a wide range of applications to digital communications and storage. Reed-Solomon codes are block codes constructed over $GF(2^m)$ of length 2^m-1 which satisfy the Singleton bound with equality. In other words, for an (n,k) RS code, the minimum distance of the code is $n-k+1$ and up to t symbol error can be corrected where $2t = n-k$. For the DSD channel, however, RS codes are not appropriate due to their fixed rate and relatively complex encoding and decoding. In order to design an RS code for a channel, the capacity of the channel must be estimated at the transmitter. For a DSD channel, a different RS code would need to be designed for each point in the room. Additionally, the number of operations to encode and decode RS codes is proportional to the data block size. This makes such codes practical for relatively small block sizes such as byte error correcting codes of length 256.

A. Rateless Codes

Rateless codes are a relatively new class of erasure correcting codes. The transmitter in this code is often termed a *digital fountain* since it emits "droplets" of data packets continuously from a given message source [16]. The receivers act as droplet collectors. Once a given receiver has enough packets the entire message can be decoded. It is not important which of the emitted packets are received, rather their number is important. As a result, these codes are termed rateless since an infinite number of independent coded packets can be generated from a given data block. Digital Fountain Inc. [17] has proposed commercial rateless codes for many erasure channels, such as packet networks, digital video distribution, software update protocols and also for file storage.

In this work, we apply a rateless code, called an *LT code* [18], to the DSD channel to approach the capacity of the channel. Originally invented by Luby, LT codes generate an infinite stream of data packets from a given data block of k packets. These packets are emitted from the moving spot of

This full text paper was peer reviewed at the direction of IEEE Communications Society subject matter experts for publication in the IEEE ICC 2006 proceedings.

the DSD emitter and collected by receivers in the room. The entire message can be decoded, with high probability, when slightly more that k packets are received [18]. LT codes are related to codes based on graphs. The transmitter packets are generated by taking the exclusive-OR of a random number of packets selected uniformly with degree selected by a robust soliton distribution [18, 19]. At the receiver, it is assumed that the degree of each packet and its interconnection is known a priori or is encoded in the header of the packet. Simplified belief propagation is applied to this graph to decode the information. The performance of the LT code depends on the degree distribution, determined by parameters c and δ, as well as on the packet size k.

The DSD system in the $6\times6\times3$ m room was simulated using a well-known LT code. The spot path was the circular path of radius 2.4. m given in Fig. 5(b). A $R = 100$ Mbps transmitter, following [10], is assumed and a spot angular speed of 10 Hz which results in a spot motion period $T = 0.1$ s. A 45° FOV, 37 pixel imaging receiver was used with identical specifications as the one presented in [10]. The receiver is located at four positions in the room as in Fig. 3. The noise and transmitted powers for the simulation were set to the values in [10] to result in BER less than 10^{-9} for the 100 Mpbs link.

A previously reported LT code with $k = 1024$, $c = 0.05$ and $\delta = 0.2$ was applied to the DSD channel [19]. Because of the small number of packets, k, this code is highly implementable and has low decoding complexity. An underlying assumption of the simulation is that the receiver has sufficient error detection ability to discard packets which are transmitted on the FOV boundary or are corrupted by noise. This encoding is done independently of the LT code in order to achieve the required BER and could be implemented using a high-speed cyclic-redundancy check code. The LT code is used to overcome the time-varying spot position of the DSD channel. Therefore, a transmitted packet is either completely received or is lost. Fig. 7 shows the distribution of needed packets for successful decoding for these parameters. Unlike RS codes, the rate of this code is not deterministic. As shown in the figure, on average 1167 packets are required to successfully decode the 1024 transmitted data packets. Define α as the average number of received packets required for successful decoding per message packet. In the case of the code with distribution presented in Fig. 7, $\alpha = 1167/1024 = 1.14$.

There are two possible scenarios under which this channel can be operated depending on whether the receiver is able to transmit a single bit of feedback to the transmitter. Consider the case where there is a single receiver in the room which is able to send a single bit of feedback to the transmitter when the current message has been correctly decoded. The feedback can occur via a diffuse optical channel (as in [20]) or using a low data rate radio channel. The transmitter will continue sending packets from a given data block until told to stop from the receiver. The average bit rate for any position in this case is

$$R_e(x, y) = \frac{C_T(x, y)R}{\alpha}$$

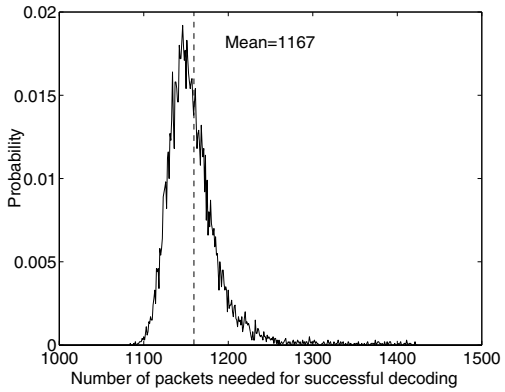

Fig. 7: Distribution of packets needed for successful decoding for $k = 1024$, $c = 0.05$, $\delta = 0.2$ over 10000 blocks.

Position	C_T	Rate without feedback	Rate with feedback
A	0.4551	12.1 Mbps	40 Mbps
B	0.3516	12.1 Mbps	30.8 Mbps
C	0.2975	12.1 Mbps	26 Mbps
D	0.1523	12.1 Mbps	13.3 Mbps

TABLE III: Achievable rates for 4 positions in room with and without a 1-bit feedback channel.

where R is the data rate of the transmitter. Table III shows simulation results for 4 different positions in the room. These rates are computed for the case that there is only one receiver in the room in each case.

If there are multiple receivers in the room, each with feedback, the transmitter will wait for acknowledgment from all receivers before proceeding to the next data block. Thus, for a group of receivers in a room, the rate is limited to that of the receiver with the smallest C_T. For example, if there are receivers at positions B and D in the room then the average rate for both of them would be 13.3 Mbps.

If the receivers are not able to transmit any feedback, it is still possible using these codes to transmit data at high bit rates to any point in the room with high reliability. Let $C_T^{\min}$ be the minimum C_T over all receivers. In this case, the transmitter sends a fixed number of packets per data block so that receivers in channels with a capacity of at least $C_T^{\min}$ can reliably receive the transmission with high probability. The packet size is set to

$$p = \frac{(C_T^{\min} TR)}{(\alpha k)}$$

so that every receiver with C_T bigger than $C_T^{\min}$ would be able to decode the whole data in one scan with high probability. Notice that the rate is independent of this packet size. The simulated rates are averages available over long term. The actual rates will fluctuate around this average. In this case, α is increased by a safety factor $\beta > 1$ to decrease the probability of decoding failure below an acceptable level. Using an overhead of 10%, i.e., $\beta = 1.1$, gives a simulated bit decoding failure on the order of 10^{-5}. Using $C_T^{\min} = 0.15$ and $\beta = 1.1$, the resulting packet size is approximately 1.75 kbits and the achievable data rate is 12.1 Mbps, as shown in Table III. Notice that the available rates also depend on the selection of packet

This full text paper was peer reviewed at the direction of IEEE Communications Society subject matter experts for publication in the IEEE ICC 2006 proceedings.

	DIFFUSE	MSD	DSD
Available Bandwidth	Low	Medium	High
Achievable Bitrate	Low	Medium	High
Transmitter Complexity	Low	High	Medium
Receiver Complexity	Low	Medium	High

TABLE IV: Comparison of DSD, MSD and Diffuse Systems.

size. Using the 85-th percentile C_T, $C_T^{\min} = 0.265$, the packet size is 3 kbits and the achievable rate for receivers equal or above the $C_T^{\min}$ is 21.1 Mbps. Thus, a rate penalty is paid for not having a single bit feedback channel from each receiver. However, with these codes significant rates are still achievable.

IV. Conclusions and Future work

In this paper, a new configuration for wireless optical networks is proposed which combines mobility and high bit rate. Unlike diffuse links where bit rate is limited by multipath dispersion, DSD channels have a multi-GHz bandwidth. Table IV compares DSD with MSD and DSD links and shows it to be complimentary to previously defined architectures.

A DSD link can be built with inexpensive translating mirrors or a rotating motor. By controlling the motor or mirror orientation and speed the DSD spot path can be adapted for individual rooms. This is unlike MSD links which require computer generated holograms [7] which must be designed for a specific location and room size. Although the transmitter design in DSD links is simpler and more flexible than MSD, DSD links have greater complexity in receiver design due to the necessity of using erasure correcting codes. We have shown in this paper that rates of 40 Mbps are possible using DSD links using only a single spot modulated at 100 Mbps.

The rates of DSD channels can be increased by either increasing the data rate of the transmitter, R, or increasing the number of spots following the path on the ceiling. For example, adding a second spot to the circular path increases complexity modestly but doubles data rates. Increasing the modulation rate of the transmitter will increase bit rates and error rates since the energy per bit is reduced. To compensate, the wide bandwidth of the DSD channel can be exploited to yield an optical power gain by trading-off bandwidth efficiency [21]. Possible modulation schemes include M-PPM and differential PPM. The DSD channel data rate is not limited by channel bandwidth but by device bandwidth. A commercial 16-element APD array is available which has about 500 MHz of bandwidth [22] and laboratory APD arrays have been shown at 8 GHz bandwidth [23]. For example, using 500 MHz transceiver with 4-PPM modulation to compensate for SNR reduction, it is possible to achieve near 400 Mbps rates.

The DSD channel is an attractive configuration for multicast indoor optical wireless networks since it is inexpensive, flexible and has a high data rate. Current work centers on the development of low complexity codes to jointly combat noise and erasure and on the implementation of an experimental DSD channel.

References

[1] F. R. Gfeller and U. Bapst, "Wireless in-house communication via diffuse infrared radiation," *Proc. IEEE*, vol. 67, no. 11, pp. 1474–1486, Nov. 1979.

[2] F. Gfeller and W. Hirt, "Advanced infrared (AIr): Physical layer for reliable transmission and medium access," in *Proc. IEEE Int. Zurich Seminar on Broadband Commun.*, 2000, pp. 77–84.

[3] R. R. Valadas, A. R. Tavares, A. M. de Oliveira Duarte, A. C. Moreira, and C. T. Lomba, "The infrared physical layer of the IEEE 802.11 standard for wireless local area networks," *IEEE Commun. Mag.*, vol. 36, no. 12, pp. 107–112, Dec. 1998.

[4] K. J. D. C. O'Brien, G. E. Faulkner, E. B. Zyambo, D. J. Edwards, M. Whitehead, P. Stavrinou, G. Parry, J. Bellen, M. J. Sibley, V. A. Lalithambika, V. M. Joyer, R. J. Samsudin, D. M. Holburn, and R. J. Mears, "High-speed intergrated transceivers for optical wireless," *IEEE Commun. Mag.*, Mar. 2003.

[5] G. Yun and M. Kavehrad, "Spot-diffusing and fly-eye receivers for indoor infrared wireless communications," *Proc of IEEE Intl. Conference on Selected Topics in Wireless Communications*, pp. 262–265, 1992.

[6] S. T. Jivkova and M. Kavehrad, "Multispot diffusing configuration for wireless infrared access," *IEEE Trans. Commun.*, vol. 48, no. 6, pp. 970–978, June 2000.

[7] M. Kavehrad and S. Jivkova, "Indoor broadband optical wireless communications:optical subsystems design and their impact on channel characteristics," *IEEE Wireless Commun. Mag.*, pp. 30–35, Apr. 2003.

[8] S. Jivkova and M. Kavehrad, "Receiver designs and channel characterization for multi-spot high-bit-rate wireless infrared communications," *IEEE Trans. Commun.*, vol. 49, no. 12, pp. 2145–2153, Dec. 2001.

[9] A. G. Al-Ghamdi and J. M. H. Elmirghani, "Line strip spot-diffusing transmitter configuration for optical wireless systems influenced by background noise and multipath dispersion," *IEEE Trans. Commun.*, vol. 52, no. 1, pp. 37–45, Jan. 2004.

[10] J. M. Kahn, R. You, P. Djahani, A. G. Weisbin, B. K. Teik, and A. Tang, "Imaging diversity receivers for high-speed infrared wireless communication," *IEEE Commun. Mag.*, pp. 88–94, Dec. 1998.

[11] J. M. Kahn and J. R. Barry, "Wireless infrared communications," *Proc. IEEE*, vol. 85, pp. 265–298, Feb. 1997.

[12] J. M. Kahn, W. J. Krause, and J. B. Carruthers, "Experimental characterization of non-directed indoor infrared channels," *IEEE Trans. Commun.*, vol. 43, no. 2/3/4, pp. 1613–1623, Feb/ March/ April 1995.

[13] J. R. Barry, J. M. Kahn, W. J. Krause, E. A. Lee, and D. G. Messerschmitt, "Simulation of multipath impulse response for indoor wireless optical channels," *IEEE J. Select. Areas Commun.*, vol. 11, no. 3, pp. 376–379, Apr. 1993.

[14] D. J. C. MacKay, *Information Theory, Inference and Learning Algorithms*. Cambridge University Press, 2004.

[15] Metrologic Instruments Inc., IS8550 HOLOTrak, `www.aoainc.com`.

[16] J. Byers, M. Luby, and M. Mitzenmacher, "A digital fountain approach to asnychronous reliable multicast," *IEEE J. Select. Areas Commun.*, vol. 20, no. 8, pp. 1528–1540, Oct. 2005.

[17] Digital Fountain Inc, `www.digitalfountain.com`.

[18] M. Luby, "LT codes," *Proceedings of the ACM Symposium on Foundations of Computer Science*, 2002.

[19] F. Uyeda, H. Xia, and A. A. Chien, "Evaluation of a high performance erasure code implemention," *Computer Science and Engineering Department, University of California, San Diego*, Sept. 2004.

[20] V. Jungnickel, A. Forck, T. Haustein, U. Kruger, V. Pohl, and C. von Helmolt, "Electronic tracking for wireless infrared communications," *IEEE Trans. Wireless Commun.*, vol. 2, no. 5, pp. 989–999, Sept. 2003.

[21] S. Hranilovic and F.R. Kschischang, " Optical intensity-modulated direct detection channels: signal space and lattice codes," *IEEE Trans. Inform. Theory*, vol. 49, no. 6, pp. 1385–1399, June 2003.

[22] Pacific Silicon Sensor Inc., AD-LA-16-9-DIL 18, Avalanche Photodiode array, `www.pacific-sensor.com`.

[23] X.G. Zheng, J.S. Hsu, J.B. Hurst, X. Li, S. Wang, X. Sun, A.L. Holmes, J.C. Campbell, A.S. Huntington and L.A. Coldren,"Long-wavelength $In_{0.53}Ga_{0.47}As - In_{0.52}Al_{0.48}As$ large-area avalanche photodiodes and arrays," *IEEE J. Quantum Electron*, vol. 40, no. 8, pp. 1068–1073, Aug 2004.

This full text paper was peer reviewed at the direction of IEEE Communications Society subject matter experts for publication in the IEEE ICC 2006 proceedings.